

Modeling of Different Tower Grounding Systems Using Hybrid Continuous Circuit-Trapezoidal Integration Method

Mohammadbagher Asadpourahmadchali¹,
Mohsen Niasati¹, Yousef Alinejad-Beromi¹

Abstract: In order to protect the transmission lines against lightning strikes, it is important to investigate the tower grounding system. In this paper, a recent method called hybrid continuous circuit-trapezoidal integration method is used to calculate the impulse impedance of the grounding system. Moreover, conventional structures of the grounding systems have been simulated and the results show that, with the same wire length, the square with additional wire system has the least impulse impedance as compared to counterpoise, square and crow's foot. Moreover, the effects of soil resistivity and lightning current rise-time on the impulse impedance of these grounding systems are investigated. It is concluded that the design of the grounding system depends on the geographic location of the site in terms of soil resistivity and isotropic characteristics of the area in terms of lightning current rise-time.

Keywords: Lightning, Grounding system modeling, Hybrid continuous circuit-trapezoidal integration method, Soil resistivity

1 Introduction

The impulse impedance of grounding systems in transmission line towers is an important parameter in lightning withstand levels of transmission lines. A determining factor in transferring lightning current, when striking to the towers or protective wires, is tower grounding systems [1]. The overvoltage produced in such situations can cause back flashover and may flow through the transmission line. The geometrical shape of the conductor and the soil resistivity are amongst the most critical factors in electrical operation of a grounding system. Exact characteristics and optimal structure of the grounding system in power frequency (50 and 60 Hz) are discussed in [2, 3], where the tower grounding system is modeled as lumped resistance. On the other hand, in transient conditions such as lightning faults, the inductive and capacitive properties of conductors play a key

¹Department of Computer and Electrical Engineering, Semnan University, Semnan, Iran;
E-mails: mb.asadpoor@semnan.ac.ir; mniasati@semnan.ac.ir; yalinejad@semnan.ac.ir

role. The modeling in these conditions is more sophisticated than that of a power frequency modeling. Also, the lightning current shape and soil frequency dependency are affective [4 – 6]. Impulse impedance is the most notable feature of the grounding system in such circumstances. It is defined as the ratio of peak voltage to peak current. Numerous methods have been proposed for transient modeling of grounding systems so far. A summary of the methods is represented as follows.

Transmission Line Method (TLM) models the grounding system similar to wave propagation in the transmission line. This method can be solved in time and frequency domains and can be implemented in numerical analysis software such as EMTP [7 – 10]. Moreover, electrical parameters in this method can be conducted by auxiliary software such as the finite element method. The coupling between the conductor segments is taken into account and the accuracy of the method is observed by comparing with experimental results. Another method is Nodal Frequency Analysis Method which examines various structures of the grounding systems in the frequency domain. However, this method is prone to errors in the Fourier Transform. Thus, the high-frequency harmonics that can miscalculate the impulse impedance is observed [11 – 14]. FDM and FEM solve Maxwell equations around the grounding conductors by establishing meshes in this volume to calculate voltage and electric field strength. Minimal simplification and good accuracy are among the benefits of this method. On the other hand, these methods are not suitable for practical applications as they are complicated and time-demanding [15 – 17]. HCCTIM is the most recent method in analyzing the grounding system, which adopts the continues circuit method and the trapezoidal integration method [18, 19]. Electrical parameters are calculated by integration rules. The accuracy of this method is verified with other experimental results and modeling methods. Due to satisfactory required time and the obtained results, the grounding system modeling in this paper employs the HCCTIM.

This paper aims at comparing four common tower grounding structures: counterpoise, crow's foot, square and square with additional wires, modeled using the HCCTIM method proposed in [18]. The validation of this method to model the mentioned structures is verified by the CDEGS software. Moreover, to compare these structures, the total length of the conductors is fixed and the impulse impedance is calculated. Also, the effects of lightning current shape properties, waveform rise time, and soil resistivity are evaluated. Based on these results, the best structure is distinguished. The combined analyses of soil resistivity and waveform rise time are also carried out.

The paper is organized as follows. In Section 2, the modeling procedure of the HCCTIM is explained. In Section 3, the validity of the HCCTIM to model the four common tower grounding structures is conducted with the CDEGS software.

In Section 4, the parameters effective on the impulse impedance of the structures are investigated. Finally, the concluding remarks are given in Section 5.

2 Modeling Details

The procedure for grounding system is based on the Continues Circuit solved with Trapezoidal Integration method as introduced below in summary.

2.1. Grounding system modeling

In the Continues Circuit method, grounding conductors are divided into small segments called dl . Fig. 1 shows the electrical parameters between two segments of a grounding system [18].

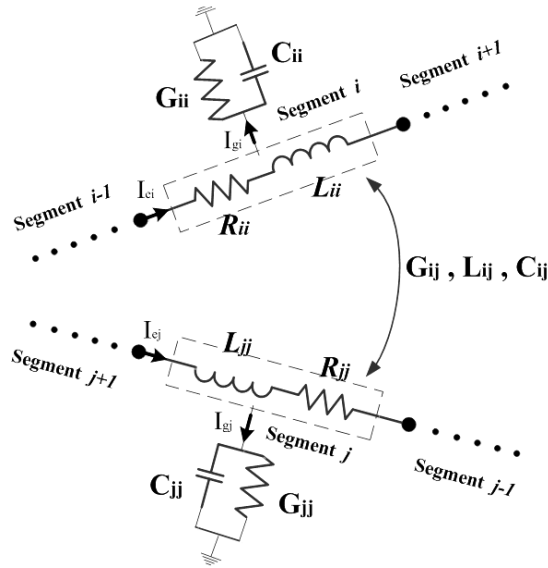


Fig. 1 – The circuit model of the grounding system.

Electrical equations, excluded from the grounding system and based on Fig. 1, are solved using the Trapezoidal Integration method [18]. Finally, the equations extracted for the voltage at node n , $V_n(t)$, the current passing through the conductor segment i , I_{ei} , and the current passing from a conductor segment to the earth, I_{gi} , are represented as follows.

$$V_n(t) = \frac{\Delta I_1 + \Delta I_2 + \Delta I_3 + \Delta I_4 + I_j(t)}{0.25A(2\Delta Y_1 + \Delta Y_2)A^T}, \quad (1)$$

where:

$$\begin{aligned}\Delta Y_1 &= \Delta t \left[R_e \frac{\Delta t}{2} - L_e \right]^{-1}, \quad \Delta Y_2 = G_e + \frac{2C_e}{\Delta t}, \\ \Delta I_1 &= A \left[R_e \frac{\Delta t}{2} - L_e \right]^{-1} R_e(\Delta t) \sum_{n=1}^{N-1} I_e(t - n\Delta t), \\ \Delta I_2 &= -A \left[R_e \frac{\Delta t}{2} - L_e \right]^{-1} A^T(\Delta t) \sum_{n=1}^{N-1} V_n(t - n\Delta t), \\ \Delta I_3 &= -0.25 |A| G_e |A|^T \sum_{n=1}^{N-1} V_n(t - n\Delta t), \\ \Delta I_4 &= 0.5 |A| \sum_{n=1}^{N-1} I_g(t - n\Delta t) + I_j(t).\end{aligned}$$

$V_n(t)$ is the node voltage at time t , $I_e(t - n\Delta t)$ denotes the electrode current at time $t - n\Delta t$, $V_n(t - n\Delta t)$ represents the node voltage at time $t - n\Delta t$ and $I_g(t - n\Delta t)$ is the ground leaking current at time $t - n\Delta t$. The unknown parameters I_e and I_g at time t are calculated in (2) and (3), respectively.

$$I_e(t) = \frac{\Delta Y_1}{\Delta t} (\Delta V_1 + \Delta V_2 + A^T V_n(t)), \quad (2)$$

where

$$\begin{aligned}\Delta V_1 &= A^T(\Delta t) \sum_{n=1}^{N-1} V_n(t - n\Delta t) \quad \text{and} \quad \Delta V_2 = -R_e(\Delta t) \sum_{n=1}^{N-1} I_e(t - n\Delta t). \\ I_g(t) &= \Delta I_1 + \Delta I_2 - 2 \sum_{n=1}^{N-1} I_g(t - n\Delta t),\end{aligned} \quad (3)$$

where

$$\Delta I_1 = 2G_e \sum_{n=1}^{N-1} V_n(t - n\Delta t) \quad \text{and} \quad \Delta I_2 = \left[G_e + \frac{2C_e}{\Delta t} \right] V_n(t).$$

2.2 Lightning current waveform modeling

The lightning current waveform is represented by the Heidler function as follows [11],

$$i(t) = \frac{I_0}{\eta} \frac{(t/\tau_1)^2}{1 + (t/\tau_1)^2} e^{-t/\tau_2}, \quad (4)$$

where, I_0 is the amplitude of the impulse current, τ_1 is the waveform rise-time, τ_2 is the 50% decay time waveform, and η is the amplitude corrector,

$$\eta = \exp\left(-(\tau_1/\tau_2)\sqrt{2(\tau_2/\tau_1)}\right).$$

The parameters to make different lightning current waveforms are presented in **Table 1**.

Table 1
Different lightning current waveform parameters (10 kA amplitude).

Waveform type [μs]	I_0 [A]	τ_1 [μs]	τ_2 [μs]
0.25/100	9930	0.0075	140
1/100	9820	0.07	170
2.6/100	9700	0.238	140
5/100	9600	0.69	135
10/100	9430	2	125

3 Validation of HCCTIM

To validate the proposed model, CDEGS software is used to simulate a counterpoise grounding system presented in Fig. 2. The CDEGS software can simulate the impulse characteristics of grounding systems in the frequency domain [20, 21]. The length, radius, and burial depth of the grounding wire are 20, 0.01 and 0.8 m, respectively. The resistivity of the soil is $150 \Omega\text{m}$ and the length of each element of the wire, (dl), is 4 m.

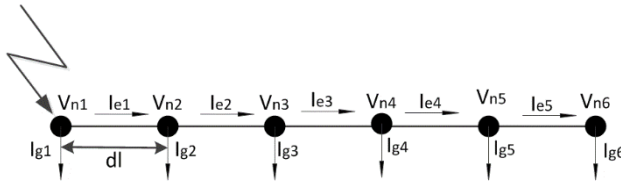


Fig. 2 – *The counterpoise grounding system segmentation.*

The current wave applied to node 1 has the characteristics of 10 KA and 2.6/100 μs as in **Table 1**. The maximum frequency of the applied current is 5.12MHz, and the minimum wavelength will be 17.1 m according to (13) [22].

$$\lambda = 3160\sqrt{\rho/f_m}. \quad (5)$$

In the above equation, ρ is the soil resistivity in Ωm , f_m is the maximum frequency of the applied current in Hz and λ is minimum wavelength in m. Equation (13) indicates the proper size of dl , 4 m, as compared to the minimum wavelength, 17.1 m. The GPR of the counterpoise grounding system calculated using the proposed method and CDEGS software is shown in Fig. 3.

In Fig. 3, the GPR calculated by CDEGS software and the proposed method is 193.5 kV and 203.6 kV, respectively. Moreover, the impulse impedance (ratio of peak voltage to peak current) calculated by CDEGS software and the proposed method is 19.4 and 20.4 Ω , respectively. The error rate for the proposed method compared to CDEGS software is 5.2%, which is calculated by (6):

$$\delta = \frac{|Z'_c - Z_c|}{Z_c} \quad (6)$$

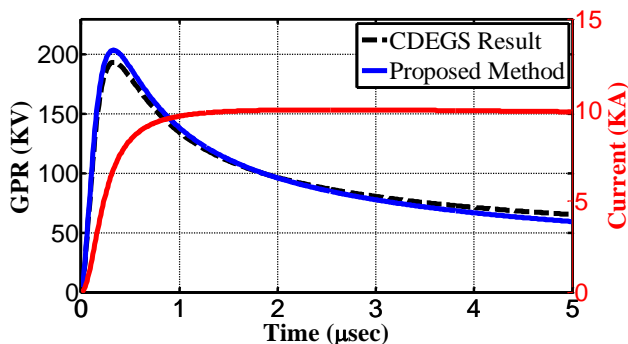


Fig. 3 – GPR of the counterpoise grounding system calculated by the proposed method and CDEGS software.

In the above equation, Z'_c and Z_c are the impulse impedance calculated by the proposed method and the CDEGS, respectively. Moreover, the resistance of the horizontal grounding system calculated by *Sunde* is 4.4 Ω [5]. Due to the neglecting the mutual coupling between the elements and the type of waveform, the *Sunde* cannot calculate the impulse impedance correctly. The final value of the impedance of the grounding system (impedance after wave tail time) calculated by the proposed method and CDEGS software is 4.8 Ω and 4.7 Ω , respectively. Therefore, the value of the impedance calculated by *Sunde* is the final impedance of the grounding system. On the other hand, the impulse impedance has the prominent factor to calculate the GPR of the grounding system when lightning current is applied.

4 Effect of Various Parameters on the Impulse Impedance

4.1 Effect of the Grounding System Structure

The flow of lightning current through the transmission line tower and its grounding system leads to the appearance of overvoltage on the insulator strings. To reduce this overvoltage, various structures have been proposed to decrease the impulse impedance of grounding system. Some common structures are

counterpoise, crow’s foot, square and square with additional wires. Fig. 4 shows these types of structures.

The impulse impedances of these structures differ in a definite condition. The first stroke lightning with a current of 10 KA and 10/100 μ s is applied to each of these structures. To better compare the impulse impedance of these four structures, the total length of the conductor in each structure is set 64 m. This means that the length of the counterpoise wire is 64 m, the length of each branch of the crow’s foot structure is 21.3 m, the length of each side of the square structure is 16 m and the length of each side and the additional wire of the square structure with additional wires are 8 m. The soil resistivity is assumed 150 Ω m and other parameters are the same as Fig. 2. The GPR of these structures is shown in Fig. 5.

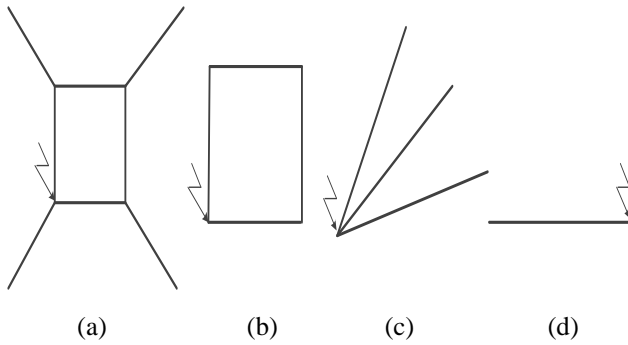


Fig. 4 – Different types of the grounding system structure: (a) Square with additional wires; (b) Square; (c) Crow’s foot and (d) Counterpoise.

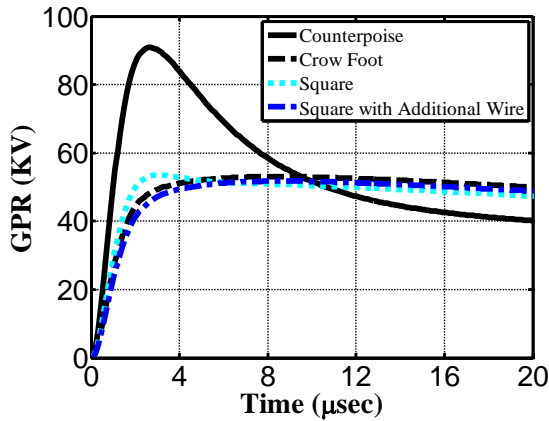


Fig. 5 – The GPR of the four mentioned structures.

According to Fig. 5, the value of the impulse impedance of the counterpoise, crow’s foot, square and square with additional wires is 9.1, 5.3, 5.4 and 5.2 Ω , respectively. As a result, the square with additional wires structure has the lowest GPR compared to the other structures with the same wire length. It can be deduced that, in this condition, except counterpoise structure, the other grounding systems have the same impulse impedance approximately.

4.2 Effect of Different Types of Lightning Current Waveform

According to IEC 62305, two types of lightning current are provided: first short stroke and subsequent short stroke [23]. The first and subsequent short strokes have a rise-time of 10 and 0.25 μs and a tail time of 350 and 100 μs , respectively. Since the rise-time has a greater impact on the impulse impedance than the tail time [24], current waveforms of 0.25, 1, 5, and 10 μs rise-time and a fixed tail time of 100 μs and a fixed amplitude of 10 KA are applied to the grounding systems. The soil resistivity is 150 Ωm and other characteristics are the same as previous section. The impulse impedances of the grounding systems are presented in **Table 2**.

The results of **Table 2** show that the impulse impedance increases with decreasing the rise-time of lightning waveform. This is duo to an increase in di/dt which increments the inductive voltage of grounding systems. It is worth noting that, according to **Table 2**, the square with additional wire has the best performance compared to other structures for all rise times.

Table 2
The impulse impedance of the grounding systems with different lightning current rise-times.

Rise-time [μs]	0.25	1	2.6	5	10
Counterpoise impulse impedance [Ω]	70.78	32.64	20.34	13.49	9.08
Crow’s foot impulse impedance [Ω]	37.81	17.00	10.61	6.86	5.30
Square impulse impedance [Ω]	42.94	19.04	11.74	7.75	5.35
Square with additional wire impulse impedance [Ω]	32.58	15.01	9.25	6.20	5.17

4.3 Effect of soil resistivity

As transmission lines pass through different locations, the soil resistivity of the tower grounding system is not the same. Therefore, the influence of different soil resistivities on the impulse impedance at different lightning current rise-times is shown in Figs. 6 and 7.

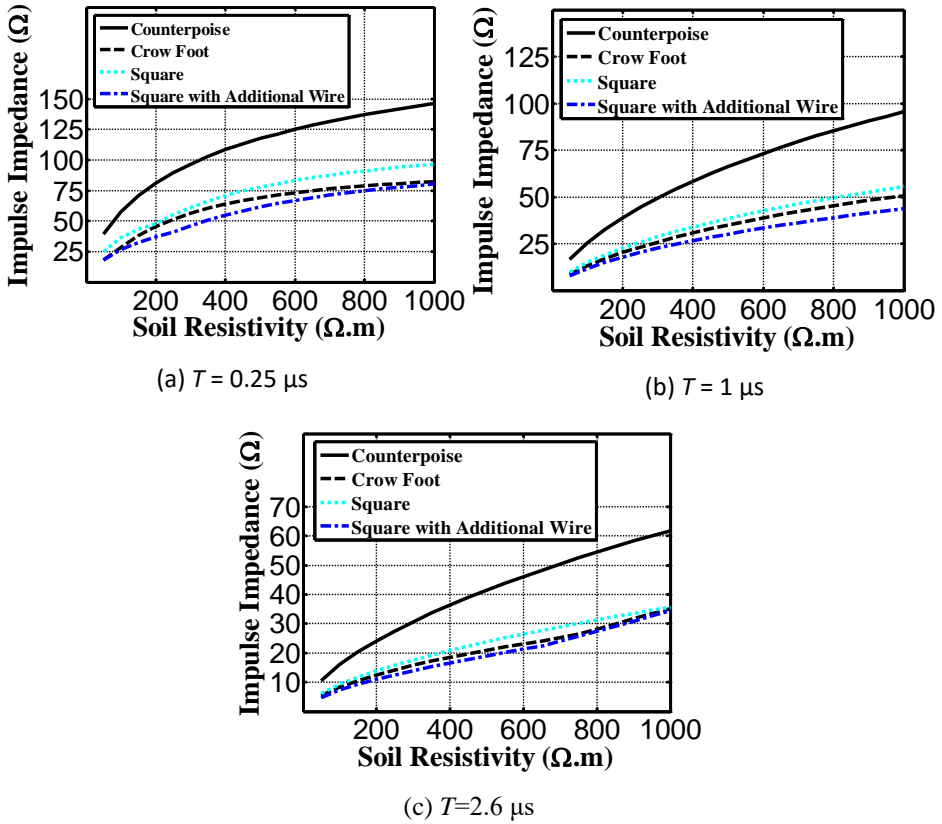


Fig. 6 – Impulse impedance of grounding systems at soil resistivity of $50 \Omega.m$ to $100 \Omega.m$ and lightning current rise-time of: (a) $0.25 \mu s$; (b) $1 \mu s$; (c) $2.6 \mu s$.

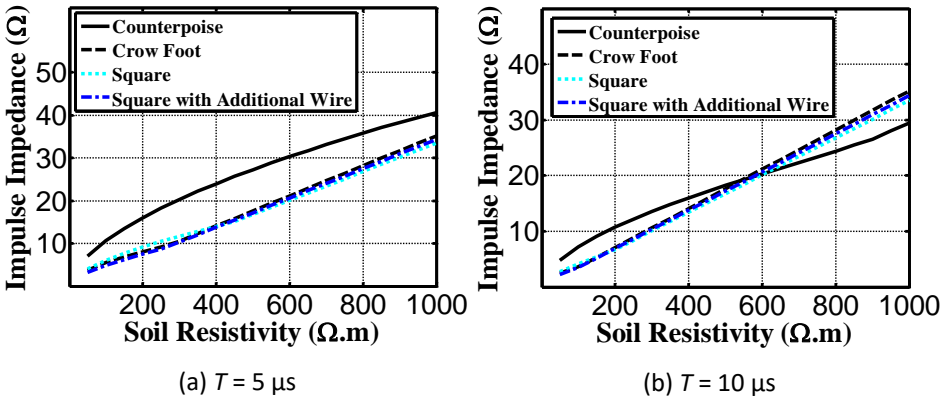


Fig. 7 – Impulse impedance of grounding systems at soil resistivity of $50 \Omega.m$ to $100 \Omega.m$ and lightning current rise-time of: (a) $5 \mu s$; (b) $10 \mu s$.

According to Fig. 6, at lightning current rise-time of 0.25, 1 and, 2.6 μs and all soil resistivities, the impulse impedance of square with additional wire structure is lower than that of other structures. For lightning current rise-time of 5 μs , Fig. 7, the crow's foot, square and, square with additional wire structures have almost the same impulse impedance, which is lower than that of the counterpoise structure. Moreover, at 10 μs lightning current rise-time, the impulse impedance of counterpoise structure is the lowest for soil resistivities greater than 600 Ωm . It can be deduced that at high soil resistivity and high lightning current rise-time, the grounding structure should have long shape (should be longer?) to show the minimum impulse impedance.

4.4 Combined Effect of Soil Resistivity and Lightning Current Rise Time

Fig. 8 shows the effect of soil resistivity and lightning current rise-time considered simultaneously. According to Fig. 8, for a ρ/T ratio of smaller than 20, the impulse of the four grounding systems are the same; for ρ/T between 20 and 56, the impulse impedance of the crow's foot, square and, square with additional wire structures are approximately the same and less than that of the counterpoise structure; for ρ/T greater than 56, the impulse impedance of square with additional wire provides the best performance compared to other structures. It can be concluded that with low rise-time or high soil resistivity, the square with additional wire structure has the lowest impulse impedance and is suggested to be adopted in tower grounding systems.

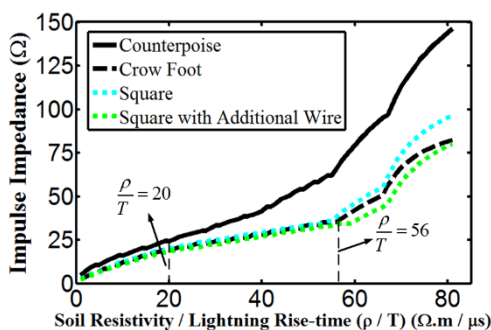


Fig. 8 – Impulse impedance of grounding systems at various soil resistivity/lightning current rise-time.

5 Conclusion

Reducing impulse impedance of the grounding system is one of the solutions to decrease the possibility of occurrence of back flashovers in overhead transmission lines. Various parameters affect the impulse impedance, such as soil resistivity, lightning current waveform rise-time and grounding system structure. In term of the type of grounding structure, four common ones, counterpoise,

crow's foot, square and square with additional wires are modeled using the recent accurate and truthful method, called HCCTIM. Also, the validity of the method is confirmed using the CDEGS software. Soil resistivity is a significant parameter due to its direct impact on the amount of leakage current flowing into the earth. As a result, at high soil resistivity (1000 Ωm), the counterpoise structure provides better performance thanks to having a longer conductor to pass the leakage current to the earth. Nonetheless, at lower soil resistivity, the square with additional wire structure is the best option. Moreover, decreasing the rise-time of lightning waveform increases the impulse impedance of the grounding system as it increases the inductance of grounding the system. In fact, in lower lightning current rise-time, higher frequencies appear in the applied current which increase the inductive impedance of grounding system. It is concluded that at low time lightning current rise-time, the square with additional wire structure has the lowest impulse impedance. However, it has been shown that the ratio of lightning current rise time and soil resistivity should be investigated in grounding system analysis at the same time. From this aspect, at a lower ratio, all of the mentioned structures present the same impulse impedance. For ratios between 20 to 56, the counterpoise structure shows a higher impulse impedance; however, other structures show the same impulse impedance value. On the other hand, at higher ratios, the square with additional wires has better performance or lower impulse impedance. In conclusion, the results show that the square with additional wire structure has the least impulse impedance compared to other conventional structures.

6 References

- [1] A.F. Otero, J. Cidras, J.L. del Alamo: Frequency-Dependent Grounding System Calculation by Means of a Conventional Nodal Analysis Technique, *IEEE Transactions on Power Delivery*, Vol. 14, No. 3, July 1999, pp. 873 – 878.
- [2] IEEE Guide for Safety in AC Substation Grounding, *IEEE Std 80-2000*, IEEE, New York, 2000.
- [3] C.- H. Lee, C.- N. Chang: Comparison of the Safety Criteria Used for Grounding Grid Design at 161/23.9-kV Indoor-Type Substation, *International Journal of Electrical Power & Energy Systems*, Vol. 49, July 2013, pp. 47 – 56.
- [4] R. Rudenberg: Grounding Principles and Practices I - Fundamental Considerations on Ground Currents, *Electrical Engineering*, Vol. 64, No. 1, January 1945, pp. 1 – 13.
- [5] E.D. Sunde: Surge Characteristics of a Buried Bare Wire, *Electrical Engineering*, Vol. 59, No. 12, December 1940, pp. 987 – 991.
- [6] B.R. Gupta, B. Thapar: Impulse Impedance of Grounding Grids, *IEEE Transactions on Power Apparatus and Systems*, Vol. PAS-99, No. 6, November 1980, pp. 2357 – 2362.
- [7] A.P. Meliopoulos, M.G. Moharam: Transient Analysis of Grounding Systems, *IEEE Transactions on Power Apparatus and Systems*, Vol. PAS-102, No. 2, February 1983, pp. 389 – 399.
- [8] F.E. Mentre, L.D. Grcev: EMTP-Based Model for Grounding System Analysis, *IEEE Transactions on Power Delivery*, Vol. 9, No. 4, October 1994, pp. 1838 – 1849.

- [9] A.C.S. de Lima, C. Portela: Inclusion of Frequency-Dependent Soil Parameters in Transmission-Line Modeling, *IEEE Transactions on Power Delivery*, Vol. 22, No. 1, January 2007, pp. 492 – 499.
- [10] D.S. Gazzana, A. S. Bretas, G.A.D. Dias, M. Telló, D.W.P. Thomas, C. Christopoulos: The Transmission Line Modeling Method to Represent the Soil Ionization Phenomenon in Grounding Systems, *IEEE Transactions on Magnetics*, Vol. 50, No. 2, February 2014, pp. 103 – 107.
- [11] B. Zhang, J. He, J.- B. Lee, X. Cui, Z. Zhao, J. Zou, S.- H. Chang: Numerical Analysis of Transient Performance of Grounding Systems Considering Soil Ionization by Coupling Moment Method with Circuit Theory, *IEEE Transactions on Magnetics*, Vol. 41, No. 5, May 2005, pp. 1440 – 1443.
- [12] A.F. Otero, J. Cidrás, C. Garrido: Frequency Analysis of Grounding Systems, *Proceedings of the 8th International Conference on Harmonics and Quality of Power*, Athens, Greece, October 1998, pp. 348 – 353.
- [13] J. Cidrás, A.F. Otero, C. Garrido: Nodal Frequency Analysis of Grounding Systems Considering the Soil Ionization Effect, *IEEE Transactions on Power Delivery*, Vol. 15, No. 1, January 2000, pp. 103 – 107.
- [14] R. Shariatinasab, P. Tadayon, A. Ametani: A Hybrid Method for Evaluating of Lightning Performance of Overhead Lines based on Monte Carlo Procedure, *Journal of Electrical Engineering*, Vol. 67, No. 4, July 2016, pp. 246 – 252.
- [15] G. Ala, P.L. Buccheri, P. Romano, F. Viola: Finite Difference Time Domain Simulation of Earth Electrodes Soil Ionization Under Lightning Surge Conditions, *IET Science, Measurement & Technology*, Vol. 2, No. 3, May 2008, pp. 134 – 145.
- [16] A. Habjanic, M. Trlep: The Simulation of the Soil Ionization Phenomenon Around the Grounding System by the Finite Element Method, *IEEE Transactions on Magnetics*, Vol. 42, No. 4, April 2006, pp. 867 – 870.
- [17] L. Qi, X. Cui, Z. Zhao, H. Li: Grounding Performance Analysis of the Substation Grounding Grids by Finite Element Method in Frequency Domain, *IEEE Transactions on Magnetics*, Vol. 43, No. 4, April 2007, pp. 1181 – 1184.
- [18] M. Asadpourahmadchali, M. Niasati, Y. Alinejad-Beromi: Hybrid Continuous Circuit-Trapezoidal Integration Method Analysis of Multi-Cross Structure of Grounding System, *IET Science, Measurement & Technology*, Vol. 14, No. 3, May 2020, pp. 292 – 302.
- [19] M. Asadpourahmadchali, M. Niasati, Y. Alinejad-Beromi: Improving Tower Grounding vs. Insulation Level to Obtain the Desired Back-Flashover Rate for HV Transmission Lines, *Electrical Power and Energy Systems*, Vol. 123, December 2020, pp. 1 – 10.
- [20] S.C. Chapra: *Applied Numerical Methods with MATLAB: for Engineers and Scientists*, 3rd Edition, McGraw-Hill Education, New York, 2011.
- [21] CDEGS, v. 10 Software, HIFREQ Module, Safe Engineering Services & Technologies Ltd., Montreal, QC, Canada, 2002.
- [22] K. Aniserowicz, T. Maksimowicz: Comparison of Lightning-Induced Current Simulations in the Time and Frequency Domains Using Different Computer Codes, *IEEE Transactions on Electromagnetic Compatibility*, Vol. 53, No. 2, May 2011, pp. 446 – 461.
- [23] International Standard, Protection against Lightning –Part 1: General principles (IEC 62305-1), 1st Edition, International Electrotechnical Commission (IEC), Geneva, 2006.
- [24] N. Harid, H. Griffiths, S. Mousa, D. Clark, S. Robson, A. Haddad: On the Analysis of Impulse Test Results on Grounding Systems, *IEEE Transactions on Industry Applications*, Vol. 51, No. 6, November 2015, pp. 5324 – 5334.